Utilizing Affine Description for Adaptive Visual Servoing

Koh Hosoda, Kyohei Ishida, and Minoru Asada

Deptartment of Adaptive Machine Systems, Osaka University

hosoda@ams.eng.osaka-u.ac.jp

Abstract

It is difficult to design feedback gains for adaptive visual sevoing because it does not have a priori knowledge on the robot system. In this paper, to make the gain scheduling easy without calibration, an affine motion description is used to derive the image features given to the adaptive visual servoing. A camera-manipulator system whose camera is mounted on the tip of the manipulator is used to track a moving target object so as to keep its view in the image plane unchanged. In such a case, some movements of the target can be described in terms of the affine motion description in the image plane. Experimental results show the validity of the proposed method.

1 Introduction

Many attempts have been taken to perform robot tasks based on visual information. Among them, visual servoing is recently receiving more attention because it uses visual information in the dynamic feedback loop to increase robustness of the closed loop system [1]. For vision-based robots, image features on the image planes are primitive descriptions of the environments. In this sense, feature-based visual servoing control is the most fundamental one for the vision-based robots in which image features are controlled to converge to the desired ones, and therefore has been focused by many researchers [2–13].

To deal with uncalibrated camera-manipulator systems in dynamic/unknown environments, some adaptive methods have been proposed. Among such methods, Hosoda and Asada have proposed an adaptive visual servoing method [14, 15]. The method has following features:

1. It does not need *a priori* knowledge on the system parameters or on the kinematic structure of the system. That is, we need not to devote ourselves to tedious calibration processes, or to separate the unknown parameters from the system equations that depends on the detailed knowledge on the kinematic structure of the system.

2. There is no restriction on applicable camera-manipulator systems : the number of cameras, kinds of image features, structure of the system (camera-in-manipulator or camera-and-manipulator), the numbers of inputs and outputs (SISO or MIMO). The proposed method is applicable to any kinds of systems.

3. The method does not intend to obtain the true parameters but to ensure asymptotical convergence of the image features to the desired values. Therefore, the estimated parameters do not necessarily converge to the true values. In [8–12], they tried to estimate the true parameters, and therefore they need their restrictions and assumptions.

Thanks to these features, the adaptive visual servoing is applicable to various kinds of image-based robot systems [14–19].

However, because the adaptive visual servoing does not have *a priori* knowledge on the robot system, it is difficult for the designer to find out which feedback gain correspond to which motion of the robot. Therefore it is difficult to design the gains.

On the other hand, utilizing the affine motion description, one can obtain image features that represent target's translation and rotation along the optical axis by transration, scaling, and the rotation in a 2D image plane, which we call *affine image features* in the following. Becase the changes of the affine image features correspond to the motions of the target with respect to the camera, the gain scheduling becomes easy *without calibration.* Therefore, one can improve the performance of the controller without losing the stabitily of the closed loop system.

In this paper, such affine image features are proposed for the adaptive visual servoing. A camera-manipulator system whose camera is mounted on the tip of the manipulator is dealt with. The task given to the system is to track a moving target object so as to keep its views in the image planes unchanged. This paper is organized as follows. First, the adaptive visual servoing method is introduced. Then, the affine image features based on the affine motion description are proposed for the visual servoing. Finally, the validity of the proposed method is shown by the experimental results.

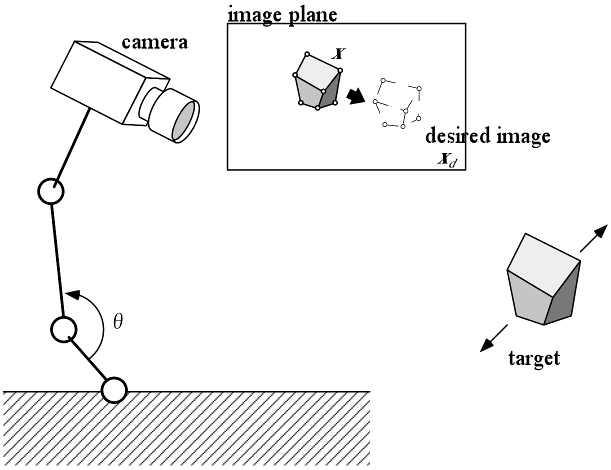

Figure 1: A camera-manipulator system

2 Adaptive visual servoing

2.1 Estimator of the relation between image features and joint angles

A camera-manipulator system whose camera is mounted on the tip of the manipulator is shown in Figure 1. From the camera, one can observe image features such as position, line length, contour length, and/or area of certain image patterns. The task of the system is to make the image features converge to the given desired values.

Let $\boldsymbol{\theta} \in \Re^n$ and $\boldsymbol{x} \in \Re^m$ denote vectors of the joint angles and the image features obtained from visual sensors, respectively. Assume that the motions of the target are slow enough with respect to those of the manipulator. A relation between $\boldsymbol{\theta}$ and $\boldsymbol{x}$ is

$$\boldsymbol{x} = \boldsymbol{x}(\boldsymbol{\theta}). \tag{1}$$

Differentiating eq.(1), we obtain a velocity relation,

$$\dot{\boldsymbol{x}} = \boldsymbol{J}(\boldsymbol{\theta})\dot{\boldsymbol{\theta}}, \tag{2}$$

where $\boldsymbol{J}(\boldsymbol{\theta}) = \partial \boldsymbol{x}/\partial \boldsymbol{\theta}^T \in \Re^{m\times n}$ is a Jacobian matrix of time-derivatives of the image features with respect to those of joint angles. This Jacobian matrix consists of on the kinematic structure of the system, the internal camera parameters such as focal length, aspect ratio, distortion coefficients, and the kinematic parameters such as the length of links and the relative position and orientation of the camera with respect to the tip of the manipulator.

Assuming that the motions of the camera-manipulator system are slow enough to consider the Jacobian matrix $\boldsymbol{J}$ to be constant during the sampling time, we obtain

$$\boldsymbol{x}(k+1) = \boldsymbol{x}(k) + \boldsymbol{J}(k)\boldsymbol{u}(k), \tag{3}$$

as a discrete model of the system, where $\boldsymbol{J}(k)$ and $\boldsymbol{u}(k)(=\dot{\boldsymbol{\theta}}\Delta T)$ denote the constant Jacobian matrix and a control input vector in k-th step during sampling rate ΔT, respectively. From eq.(3), i-th row vector of the matrix $\boldsymbol{J}$, ${\boldsymbol{j}_i}^T$, is estimated as

$$\begin{aligned} &\widehat{\boldsymbol{j}}_i(k+1) - \widehat{\boldsymbol{j}}_i(k) = \\ &\frac{\{\boldsymbol{x}(k+1) - \boldsymbol{x}(k) - \widehat{\boldsymbol{J}}(k)\boldsymbol{u}(k)\}_i}{\rho_i + \boldsymbol{u}(k)^T\boldsymbol{W}_i(k)\boldsymbol{u}(k)}\boldsymbol{W}_i(k)\boldsymbol{u}(k), \end{aligned} \tag{4}$$

where ρ_i is an appropriate positive constant that makes the iteration (4) stable. When $\parallel \boldsymbol{u} \parallel$ tends to 0, the denominator tends to ρ_i and the stability is ensured even if the numerator does not tend to 0 because of disturbances. The positive constant ρ_i is determined so small that ρ_i can be neglected with respect to $\parallel \boldsymbol{u} \parallel$ when $\parallel \boldsymbol{u} \parallel$ is large. Note that when ρ is in the range $0 < \rho \leq 1$ and the matrix $\boldsymbol{W}_i$ is a covariance matrix, the proposed estimator is equivalent to the least-mean-square method [20].

The proposed estimator is intended not to obtain the true Jacobian matrix/parameters, but to estimate a matrix that satisfies eq.(3). This is the main difference from [9], [10], and [11], in which they tried to estimate the true parameters. To estimate the true parameters, one have to make restrictions and assumptions on the camera-manipulator system. The proposed estimator, however, is not intended to estimate the true parameters, but to make the closed loop system consisting of this estimator and a controller stable. Therefore, there is neither restrictions nor assumptions on the camera-manipulator system.

2.2 Adaptive visual servoing controller

The aim of the controller is to ensure convergence of the image feature vector $\boldsymbol{x}(k)$ to the desired vector $\boldsymbol{x}_d(k)$. From eq.(3), we can derive a feedforward/feedback controller,

$$\begin{aligned} \boldsymbol{u}(k) \;=\;& \widehat{\boldsymbol{J}}(k)^+\{\boldsymbol{x}_d(k+1) - \boldsymbol{x}_d(k)\} \\ &+\{\boldsymbol{I}_n - \widehat{\boldsymbol{J}}(k)^+\widehat{\boldsymbol{J}}(k)\}\boldsymbol{k}_r \\ &+\widehat{\boldsymbol{J}}(k)^+\boldsymbol{K}\{\boldsymbol{x}_d(k+1) - \boldsymbol{x}(k)\}, \end{aligned} \tag{5}$$

where $\widehat{\boldsymbol{J}}(k)^+$, $\boldsymbol{I}_n$, and $\boldsymbol{K}$ denote a pseudo-inverse matrix of $\widehat{\boldsymbol{J}}(k)$, an $n\times n$ identity matrix, and a positive-definite gain matrix, respectively. Let $\boldsymbol{k}_r$ be an arbitrary vector.

The first and second terms on the right-hand side are feedforward terms. The second term on the right-hand side denotes the redundancy of the camera-manipulator system. The third term on the right-hand side is a feedback term that ensures stability of the closed loop system.

We have proposed an adaptive visual servoing method consisting of the proposed estimator and controller shown in Figure 2.

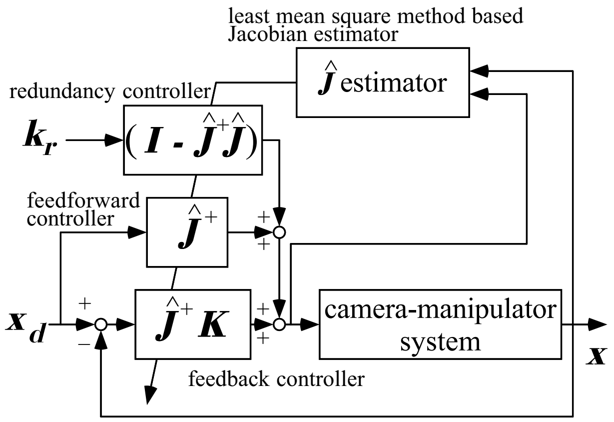

Figure 2: Block diagram of the adaptive visual servoing

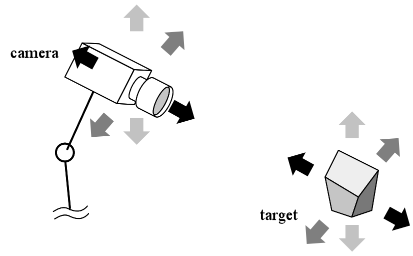

case (a) : The target translates.

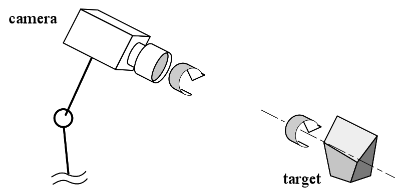

case (b) : The target rotates along the optical axis.

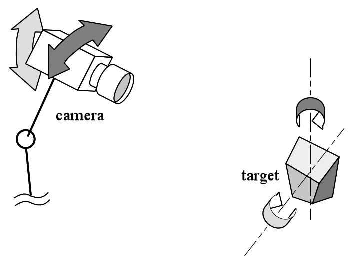

case (c) : The target rotates along the other axes.

Figure 3: Motions of the target and the camera

3 Image features based on affine motion description

The adaptive visual servoing method can deal with various quantities of image features such as position, line length, contour length, and/or area of certain image patterns. If we use coordinates of the feature points as image features for the adaptive visual servoing controller, it could be difficult to schedule feedback gains without reconstructing 3D structure.

In this section, image features based on the affine motion description are proposed for the adaptive visual servoing method. The proposed image features can make the gain scheduling easier without calibration, and therefore the performance of the method can be improved.

3.1 Motions of the target and corresponding motions of the camera

A camera-manipulator system whose camera is mounted on the tip of the manipulator is dealt with in this paper (Figure 3). When the target translates in 3D space (Figure 3 (a)), corresponding view changes in the image plane are translations and a scaling motion (Figure 4 (A)). When the target rotates along the optical axis in 3D space (Figure 3 (b)), a corresponding view is a rotation in the image plane (Figure 4 (B)). The camera motions to keep the target views unchanged are as large as those of the target in such cases (a) and (b). On the other hand, when the target rotates along other axes (Figure 3 (c)), the view changes in the image plane are such distortional motions shown in Figure 4 (C). In such cases, the camera motions to keep the target views unchanged are much larger than those of the target (see Figure 3 (c)).

From these facts, to improve the performance of the controller without losing the stability, one have to design larger gains for the motions (a) and (b) than those for (c). However, because the adaptive visual servoing does not have *a priori* knowledge on the robot system, it is difficult for the designer to find out which feedback gain corresponds to which motion of the robot as far as one use coordinates of the image feature position without reconstructing 3D structure of the system.

On the other hand, such translations and rotation as (a) and (b) are known to be described by utilizing the affine motion description. Therefore, by utilizing the affine image features that are derived by the affine motion description, one can easily schedule the gains to improve the performace.

3.2 Image features based on affine motion description

Let vectors $\boldsymbol{x}_i$ and $\boldsymbol{x}_{id}$ be a coordinate vector of an image feature point i and its desired vector, respectively. When the parallel is preserved, there is a relation between $\boldsymbol{x}_i$ and $\boldsymbol{x}_{id}$ for all i,

$$\boldsymbol{x}_i = \boldsymbol{A}\boldsymbol{x}_{id} + \boldsymbol{d}, \tag{6}$$

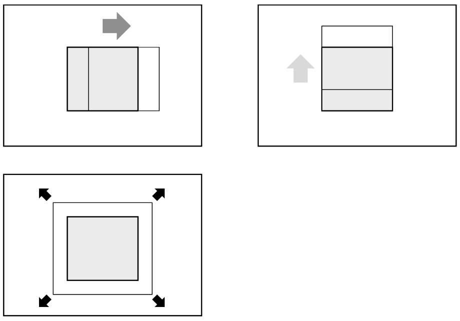

(A) : The target translates.

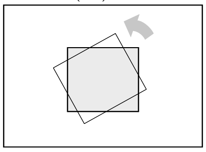

(B) : The target rotates along the optical axis.

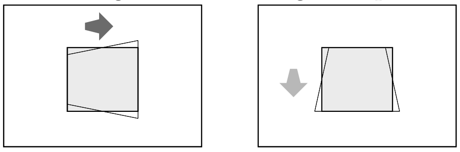

(C) : The target rotates along the other axes.

Figure 4: Corresponding view changes to the motions of the target

which is the affine motion description. Here the matrix $\boldsymbol{A} \in \Re^{2\times 2}$ consists of magnification and rotation,

$$\boldsymbol{A} = \begin{bmatrix} \lambda & 0 \\ 0 & \lambda \end{bmatrix} \begin{bmatrix} \cos\phi & \sin\phi \\ -\sin\phi & \cos\phi \end{bmatrix}. \tag{7}$$

The vector $\boldsymbol{d} \in \Re^2$ denotes a translational motion. Gathering eq.(7) for all $m/2$ image feature points, we get

$$\boldsymbol{X} = \widetilde{\boldsymbol{X}}_d \boldsymbol{B}, \tag{8}$$

where

$$\begin{aligned} \boldsymbol{X} &\triangleq \begin{bmatrix} \boldsymbol{x}_1{}^T \\ \dots \\ \boldsymbol{x}_n{}^T \end{bmatrix} \in \Re^{m/2\times 2}, \\ \widetilde{\boldsymbol{X}}_d &\triangleq \begin{bmatrix} 1 & \boldsymbol{x}_{1d}{}^T \\ \dots & \dots \\ 1 & \boldsymbol{x}_{nd}{}^T \end{bmatrix} \in \Re^{m/2\times 3}, \\ \boldsymbol{B} &\triangleq \begin{bmatrix} \boldsymbol{d}^T \\ \boldsymbol{A}^T \end{bmatrix} \in \Re^{3\times 2}. \end{aligned}$$

From eq.(8), we can estimate the matrix $\boldsymbol{B}$ by the least mean square method,

$$\boldsymbol{B} = \left(\widetilde{\boldsymbol{X}}_d{}^T \widetilde{\boldsymbol{X}}_d\right)^{-1} \widetilde{\boldsymbol{X}}_d{}^T \boldsymbol{X}. \tag{9}$$

The translational motions of the object perpendicular to the optical axis are represented by $\boldsymbol{d}$. The rotational motion along the optical axis ϕ and the magnification λ are calculated from the matrix $\boldsymbol{A}$,

$$\begin{aligned} \lambda &= \sqrt{\det(\boldsymbol{A})}, & (10) \\ \sin\phi &= (a_{12} - a_{21})/(2\lambda), & (11) \\ \cos\phi &= (a_{11} + a_{22})/(2\lambda). & (12) \end{aligned}$$

From eqs.(9), (10), (11) and (12), we can obtain image features based on affine motion description, $\boldsymbol{x}_a \triangleq [d_x, d_y, \lambda, \phi]$ from the coordinates of the image feature points $\boldsymbol{x}$. Here, we define $\boldsymbol{x}_a$ as an *affine image feature vector.*

3.3 Combination of affine features and image coordinates

Feeding the affine image features to the adaptive visual servoing, one can make a servoing controller. The task for the robot system is to keep the views of the target unchanged, therefore the controller does not have the feedforward terms of eq.(5),

$$\boldsymbol{u} = \widehat{\boldsymbol{J}}_a{}^+ \boldsymbol{K}_a(\boldsymbol{x}_{ad} - \boldsymbol{x}_a) + (\boldsymbol{I}_n - \widehat{\boldsymbol{J}}_a{}^+ \widehat{\boldsymbol{J}}_a)\boldsymbol{k}_r, \tag{13}$$

where $\widehat{\boldsymbol{J}}_a \in \Re^{n\times 4}$, $\boldsymbol{K}_a \in \Re^{4\times 4}$ and $\boldsymbol{x}_{ad} \in \Re^4$ denote the Jacobian matrix that describes the relation between the joint velocities and the time-derivatives of the affine image features, a feedback gain matrix and the desired affine image features, respectively.

Using the controller eq.(13), one can only realize the motions that are described by the affine motion description. To ensure the convergence of the view, we proposed to add terms to make the coordinates of the image points to the controller converge to the desired values utilizing the redundancy term of eq.(13) :

$$\begin{aligned} \boldsymbol{u} = \; & \widehat{\boldsymbol{J}}_a{}^+ \boldsymbol{K}_a(\boldsymbol{x}_{ad} - \boldsymbol{x}_a) \\ & + (\boldsymbol{I}_n - \widehat{\boldsymbol{J}}_a{}^+ \widehat{\boldsymbol{J}}_a)\{\widehat{\boldsymbol{J}}_x(\boldsymbol{I}_n - \widehat{\boldsymbol{J}}_a{}^+ \widehat{\boldsymbol{J}}_a)\}^+ \\ & \{\boldsymbol{K}_x(\boldsymbol{x}_d - \boldsymbol{x}) - \widehat{\boldsymbol{J}}_x \widehat{\boldsymbol{J}}_a{}^+ \boldsymbol{K}_a(\boldsymbol{x}_{ad} - \boldsymbol{x}_a)\}, \end{aligned} \tag{14}$$

where $\widehat{\boldsymbol{J}}_x \in \Re^{n\times m}$ and $\boldsymbol{K}_x \in \Re^{m\times m}$ denote the Jacobian matrix that describes the relation between the joint velocities and the velocities of image feature points and a feedback gain matrix, respectively. The block diagram of the proposed method (14) is shown in Figure 5.

By setting the gain $\boldsymbol{K}_a$ larger than $\boldsymbol{K}_x$, we can realize a high performance along the affine describable axes and stable performance along other axes.

4 Experiments

To show the validity of the proposed method, some experimental results are shown in this section.

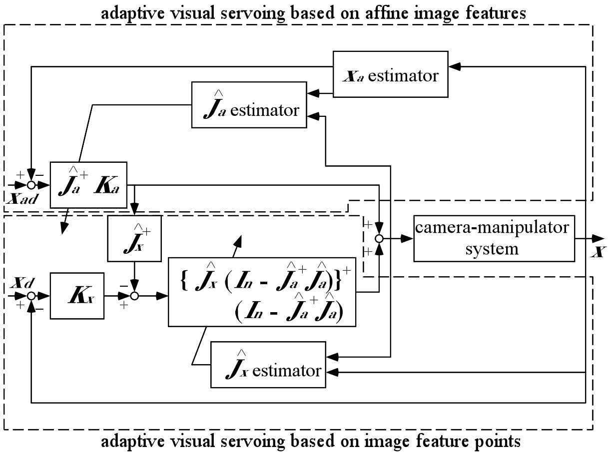

Figure 5: Block diagram of the proposed method

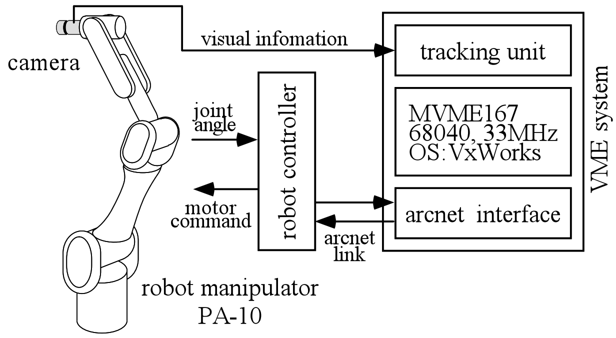

Figure 6: Experimental equipment

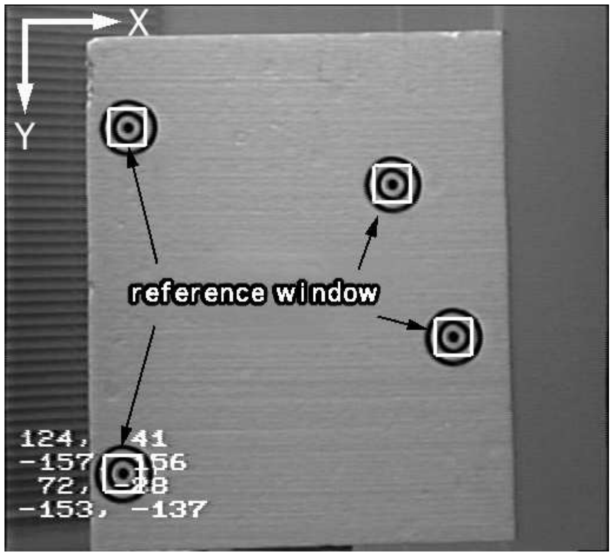

Figure 7: A view captured by the camera

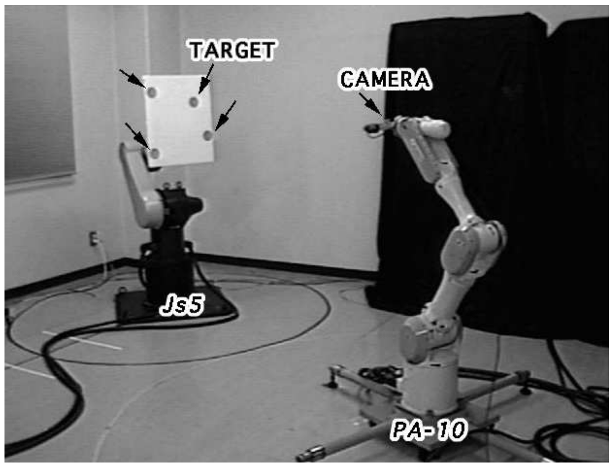

Figure 8: Overview of the experimental system

4.1 Robot system used for the experiments

In figure 6, a camera-manipulator system used for experiments is shown. Video signal from a CCD camera is sent to a tracking unit equipped with a high-speed correlation processor by Fujitsu [21](image size : 512[pixel] $\times$ 512[pixel]). We specify certain regions in the image (called templates) which we want the unit to track, before starting an experiment (see Figure 7). During the experiments the unit feeds coordinates where the distortion value SAD (Sum of Absolute Difference) is the smallest with respect to the templates to the main control board MVME167 (CPU:68040, 33MHz, Motorola). The control board calculates control signals for the manipulator by the proposed method and sends them to the manipulator controller via network(5Mbps). We use a 7 degree-of-freedom manipulator PA–10 (Mitsubishi Heavy Industry Co.). Using this experimental equipment and writing programs using C language on VxWorks (Wind River), sampling rate of the visual servoing control is 33[ms]. Distance between the manipulator and the target is approximately 2[m]. The overview of the experimental system is shown in Figure 8.

4.2 Experimental results

As we assumed that the adaptive visual servoing does not have any *a priori* knowledge on the robot system, we use arbitrary matrices for the initial matrices $\widehat{\boldsymbol{J}}_a(0)$ and $\widehat{\boldsymbol{J}}_x(0)$,

$$\widehat{\boldsymbol{J}}_a(0) = \begin{bmatrix} 5 & 0 & 0 & 5 & 0 & 1 \\ 0 & -5 & -1 & 1 & -5 & 1 \\ 1 & 1 & 1 & 1 & 0 & 2 \\ -5 & 1 & 1 & 1 & 1 & 1 \end{bmatrix}$$

$$\widehat{\boldsymbol{J}}_x(0) = \begin{bmatrix} 1 & 0 & 0 & 1 & 0 & 1 \\ 0 & -1 & -1 & 1 & -1 & 1 \\ 2 & 0 & 0 & 1 & 0 & 2 \\ 0 & -2 & -1 & 1 & -1 & 2 \\ 3 & 0 & 0 & 1 & 0 & 1 \\ 0 & -3 & -1 & 3 & -1 & 1 \\ 4 & 0 & 0 & 4 & 0 & 1 \\ 0 & -4 & -1 & 1 & -4 & 1 \end{bmatrix}$$

The forgetting factor ρ_i and the weighting matrices $\boldsymbol{W}_i$ are selected 1.0 and identical matrices, respectively. The feedback gain matrix for the affine image features $\boldsymbol{K}_a$ and that of coordinates of image feature points $\boldsymbol{K}_x$ are diag $[\ 0.03\ 0.03\ 0.8\ 1.5\ ]$ and diag$[\ 0.001\ \cdots\ 0.001\ ]$, respectively, which are selected in a trial and error manner. Using the proposed method, the gain scheduling is easy because they correspond to the motions of the camera. We also can find that the feedback gains for the affine image features are larger than those for the image feature points.

The movement of the target is as follows:

1. From $t = 4$[s] to $t = 17$[s], it moves horizontally rightward 0.25[m] and comes back to the initial posture.

2. From $t = 27$[s] to $t = 36$[s], it moves vertically upward 0.20[m] and comes back to the initial posture.

3. From $t = 46$[s] to $t = 52$[s], it rotates along the optical axis 10[deg] and comes back to the initial posture.

4. From $t = 62$[s] to $t = 74$[s], it moves along the optical axis 0.10[m] and comes back to the initial posture.

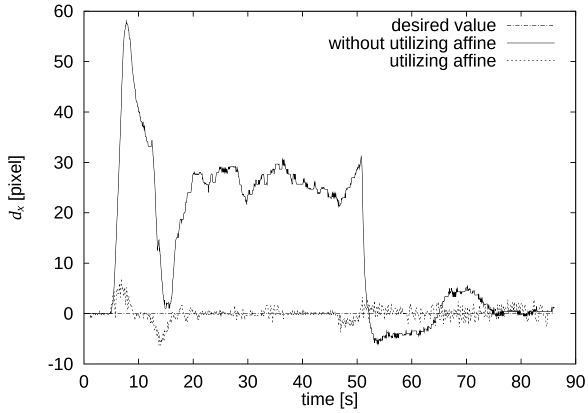

Figure 9: Experimental result (1) : affine image feature $\boldsymbol{d}_x$

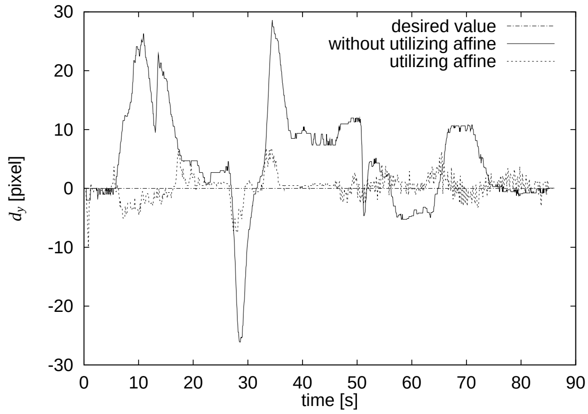

Figure 10: Experimental result (2) : affine image feature $\boldsymbol{d}_y$

In Figures 9, 10, 11, and 12, experimental results are shown, in which we can find the effectiveness of the proposed method.

5 Conclusion

In this paper, some movements of the target are described in terms of the affine motion description in the image plane. By using the affine image features for the adaptive visual servoing, scheduling of the feedback gains becomes easier because the designer can easily understand the correspondence of the affine image features to the motions of the camera.

To schedule gains is a big problem for designing the feedback loop. When the adaptive visual servoing is used, one can hardly understand the correspondance between the gains and the motions without reconstructing 3D structure of the system. By utilizing affine image features, however, one can easily understand the correspondance without 3D reconstruction.

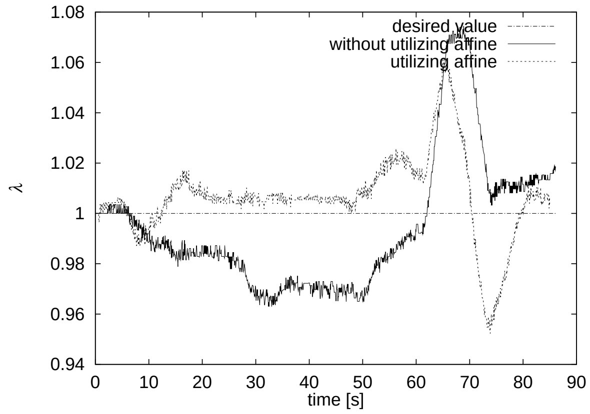

Figure 11: Experimental result (3) : affine image feature *lambda*

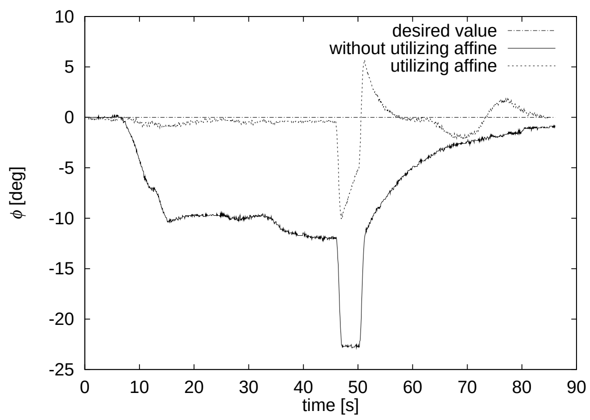

Figure 12: Experimental result (4) : affine image feature ϕ

References

[1] P. I. Corke. Visual control of robot manipulators – a review. In *Visual Servoing*, pp.1–31. World Scientific, 1993.

[2] W. Jang and Z. Bien. Feature-based visual servoing of an eye-in-hand robot with improved tracking performance. In *Proc. of IEEE Int. Conf. on Robotics and Automation*, pp.2254–2260, 1991.

[3] K. Hashimoto, T. Kimoto, T. Ebine, and H. Kimura. Manipulator control with image-based visual servo. In *Proc. of IEEE Int. Conf. on Robotics and Automation*, pp.2267–2272, 1991.

[4] N. Maru, H. Kase, et al. Manipulator control by visual servoing with the stereo vision. In *Proc. of the 1993 IEEE/RSJ Int. Conf. on Intelligent Robots and Systems*, pp.1865–1870, 1993.

[5] P. Allen, A. Timcenko, B. Yoshimi, and P. Michelman. Automated tracking and grasping of a moving object with a robotic hand-eye system. *IEEE Trans. on Robotics and Automation*, RA–9, No. 2, pp.152–165, 1993.

[6] A. Castano and S. Hutchinson. Visual compliance: Task-derected visual servo control. *IEEE Trans. on Robotics and Automation*, 10(3):334–342, 1994.

[7] G. D. Hager, W.-C. Cang, and A. S. Morse. Robot feedback control based on stereo vision: Towards calibration-free hand-eye coordination. In *Proc. of IEEE Int. Conf. on Robotics and Automation*, pp.2850–2856, 1994.

[8] L. E. Weiss, A. C. Sanderson, and C. P. Neuman. Dynamic sensor-based control of robots with visual feedback. *IEEE J. of Robotics and Automation*, RA-3, No. 5, pp.404–417, 1987.

[9] J. T. Feddema and C. S. G. Lee. Adaptive image feature prediction and control for visual tracking with a hand-eye coordinated camera. *IEEE Trans. on System, Man, and Cybernetics*, Vol. 20, No. 5, pp.1172–1183, 1990.

[10] N. P. Papanikolopoulos and P. K. Khosla. Adaptive robotic visual tracking: Theory and experiments. *IEEE Trans. on Automatic Control*, Vol. 38, No. 3, pp.429–445, 1993.

[11] B. Nelson, N. P. Papanikolopoulos, and P. K. Khosla. Visual servoing for robotic assembly. In *Visual Servoing*, pp.139–164. World Scientific, 1993.

[12] N. P. Papanikolopoulos, B. Nelson, and P. K. Khosla. Six degree-of-freedom hand/eye visual tracking with uncertain parameters. In *Proc. of IEEE Int. Conf. on Robotics and Automation*, pp.174–179, 1994.

[13] B. H. Yoshimi and P. K. Allen. Alignment using an uncalibrated camera system. *IEEE Trans. on Robotics and Automation*, Vol. 11, No. 4, pp.516–521, 1995.

[14] K. Hosoda and M. Asada. Versatile visual servoing without knowledge of true jacobian. In *Proc. of the 1994 IEEE/RSJ Int. Conf. on Intelligent Robots and Systems*, pp.186–193, 1994.

[15] K. Hosoda and M. Asada. Adaptive visual servoing for various kinds fo robot systems. In *Preprints of 5th International Symposium on Experimental Robotics*, pp.451–462, 1997.

[16] K. Hosoda, K. Sakamoto, and M. Asada. Trajectory generation for obstacle avoidance of uncalibrated stereo visual servoing without 3d reconstruction. In *Proc. of the 1995 IEEE/RSJ Int. Conf. on Intelligent Robots and Systems*, pp.29–34, 1995.

[17] K. Hosoda, K. Igarashi, and M. Asada. Adaptive hybrid visual servoing/force control in unknown environment. In *Proc. of the 1996 IEEE/RSJ Int. Conf. on Intelligent Robots and Systems*, pp.1097–1103, 1996.

[18] K. Hosoda, M. Kamado, and M. Asada. Vision-based servoing control for legged robots. In *Proc. of IEEE Int. Conf. on Robotics and Automation*, pp.3154–3159, 1997.

[19] K. Hosoda, T. Miyashita, S. Takeuchi, and M. Asada. Adaptive visual servoing for legged robots –vision-cued swaying of legged robots in unknown environments–. In *Proc. of the 1997 IEEE/RSJ Int. Conf. on Intelligent Robots and Systems*, to appear, 1997.

[20] P. Eykhoff. *System Identification*, chapter 7. John Wiley & Sons Ltd., 1974.

[21] M. Inaba, T. Kamata, and H. Inoue. Rope handling by mobile hand-eye robots. In *Proc. of Int. Conf. on Advanced Robotics*, pp.121–126, 1993.